

# Entanglement criteria for noise resistance of two-qudit states

Arijit Dutta<sup>a</sup>, Junghee Ryu<sup>b,a,\*</sup>, Wiesław Laskowski<sup>a</sup>, Marek Żukowski<sup>a</sup>

<sup>a</sup>*Institute of Theoretical Physics and Astrophysics, University of Gdańsk, 80-952 Gdańsk, Poland*

<sup>b</sup>*Centre for Quantum Technologies, National University of Singapore, 3 Science Drive 2, 117543 Singapore, Singapore*

## Abstract

Noise affects production and transmission of entanglement. We use a handy approach for a noise resistance of entanglement of two-qudit systems. A geometric concept using correlation tensors of separable and entangled states is implemented to formulate entanglement criterion. We apply the criterion to the various types of noise (white, colored, local depolarizing and amplitude damping) admixtures with the initial (pure) state. We also study the noise resistance with respect to the violation of specific family of Bell inequalities (CGLMP). A broad set of numerical and analytical results is presented.

*Keywords:* Noise resistance, Entanglement indicator, Correlation tensor

*PACS:*

## 1. Introduction

Detection of entanglement is a fundamental problem in quantum information. Many theoretical works have been done to establish a criterion to identify multipartite entanglement [1, 2, 3, 4, 5, 6, 7]. Although not all of these works have direct impact on experiments, still they provide a mathematical background to understand the phenomena.

An arbitrary density operator for two qudits can be written as

$$\rho = \frac{d-1}{2d} \left[ M_0 \otimes M_0 + \sum_{i,j=1}^{d^2-1} T_{ij} M_i \otimes M_j + (d-1) \sum_{i=1}^{d^2-1} (T_{0i} M_0 \otimes M_i + T_{i0} M_i \otimes M_0) \right],$$

where  $T_{ij}$ ,  $T_{0i}$ ,  $T_{i0}$  are components of the correlation tensor  $\hat{T}$ , and  $M_i$  ( $i \neq 0$ ) are the generalized Gell-Mann matrices (see Appendix A for details) with  $M_0 = \sqrt{\frac{2}{d(d-1)}} \mathbb{1}_d$ . The components  $T_{ij}$  are real and given by  $T_{ij} = c(d) \text{Tr}[\rho(M_i \otimes M_j)]$ , where the coefficient  $c(d)$  depends on the dimensionality (see Appendix B).

In Ref. [8], it has been shown that the correlation tensor could be utilized to construct entanglement indicators. The resulting indicators are in the form of nonlinear conditions (we will show a detailed form in the next section), thus such indicators allow detection of entanglement in more classes of quantum states than linear entanglement witnesses. The study of [8] was mainly done for multi-qubit systems. Here, we consider pairs of systems, more

complicated than qubits. In our approach we do not study the dynamics of noise, but we concentrate on properties of the state after evolving through a noisy channel. The white noise usually arises due to imperfections in experimental set up, while a colored noise can appear when multi-particle entanglement is produced via multiple emissions [9, 10]. We also analyze the effects of different local noises, modeling random environment and dissipative process [11].

A study of this kind was done for qubits in Ref. [12]. Here, we study higher dimensions. We find that in some cases there exist significant differences for noise resistances of entanglement after transferring via various noisy channels. Note that a different approach to obtain the criterion of separability of entangled qutrits in noisy channel is given in [13].

Another way to certify entanglement is to violate Bell inequalities [14]. To this end, we consider Collins-Gisin-Linden-Massar-Popescu (CGLMP) inequality of arbitrary dimension  $d$  [15]. We calculate critical noise values to vanish a violation of the inequality for noisy entangled states. We also discuss the fidelity between the initial states and the states which are parametrized by the critical noise values.

Finally, we compare difference of critical noise values between the detection of entanglement and the violation of CGLMP inequality. Such difference or gap is known as Werner gap [16, 17]. It points to the fact that the notions of entanglement detection and violations of Bell inequalities are not entirely equivalent. One can see the disparity between them in which one deals with noise admixture to the pure entangled states.

\*Corresponding author

Email address: rjhui82@gmail.com (Junghee Ryu)

## 2. Simplified entanglement condition

Separable states can be described by a fully separable extended correlation tensor,  $\hat{T}^{\text{sep}} = \sum_i p_i \hat{T}_i^{\text{prod}}$ , where  $\hat{T}_i^{\text{prod}} = \hat{T}_i^1 \otimes \hat{T}_i^2$ , and each  $\hat{T}_i^k$  is the  $d^2$ -dimensional generalized Bloch vector of  $k$ th single qudit subsystem. To obtain entanglement conditions we employ a geometrical approach based on correlation functions, which was introduced in Ref. [8]. The criterion has the following: the state  $\rho$  described by its correlation tensor  $\hat{T}$  is entangled, if

$$\max_{\hat{T}^{\text{prod}}} (\hat{T}, \hat{T}^{\text{prod}}) < (\hat{T}, \hat{T}) = \|\hat{T}\|^2. \quad (1)$$

The scalar product may be defined in various ways, provided it satisfies all required axioms. However, the simplest choice is

$$(\hat{X}, \hat{Y}) = \sum_{i,j=1}^{d^2-1} X_{ij} Y_{ij}. \quad (2)$$

In such a case, the maximum of the left-hand side of (1) can be obtained by the highest generalized Schmidt coefficient of the correlation tensor  $\hat{T}$  as

$$T_{\max} = \max_{\vec{m}_1, \vec{m}_2} (\hat{T}, \vec{m}_1 \otimes \vec{m}_2), \quad (3)$$

where  $\vec{m}_k$  is a  $(d^2-1)$ -dimensional generalized Bloch vector which describes a quantum state of  $k$ th subsystem. Note that, for  $d > 2$  we do not have a Bloch sphere. Thus  $\vec{m}_k$ 's represent the admissible Bloch vectors which represent a physical state. One can also take the maximum of the left-hand side of (1) as the square root of the highest eigenvalue of  $TT^\dagger$ , denoted by  $L_{\max}$ . However, note that  $L_{\max} \geq T_{\max}$ , and this estimate gives a less robust criterion for entanglement. Still it is technically much easier, and thus we shall use it.

Note that, the criterion is based on correlations of measurements and local measurements are enough to detect entanglement. This makes the method experimentally accessible. Moreover, as we shall see below, for some cases our entanglement indicators require fewer local measurements, not full measurement settings (i.e., no necessity of the reconstruction for the density matrix). In that sense it is more efficient scheme than a full state tomography.

## 3. Basic aims

We analyze entanglement of bipartite quantum states which are initially pure. For technical reasons we always put them in the Schmidt form:

$$|\psi\rangle = \sum_{i=0}^{d-1} c_i |ii\rangle. \quad (4)$$

We study various noisy channels, i.e., white, product, colored, local depolarizing and amplitude damping. In some cases, one can define a critical parameter  $v_{\text{crit}}$  for the noisy

output, of the form  $\rho(v) = v|\psi\rangle\langle\psi| + (1-v)\rho_{\text{noise}}$ , such that for  $v > v_{\text{crit}, ENT}^d$  the state  $\rho(v)$  is entangled. The action of a channel on a density matrix of two-qudit can also be written in terms of its operation elements, more precisely  $\rho \rightarrow \sum_{u,v} E_u(p) \otimes E_v(p) \rho (E_u(p) \otimes E_v(p))^\dagger$ , where  $E_l$  is an operation element of the channel parametrized by  $p$ , a certain strength parameter to be specified later. We define this parametrization as  $p = 1$  defines no noise, just unitary (local) evolution, while  $p = 0$  signifies the maximally noisy state leaving the channel. Hence, one can show presence of entanglement by satisfying the condition  $p > p_{\text{crit}, ENT}^d$ . Thus such a description is a generalization of the one involving  $v_{\text{crit}}$ . We also introduce a quantity

$$\xi(p_{\text{crit}, ENT}^d) = \min \left[ \left( \frac{\|\hat{T}(p_{\text{crit}, ENT}^d)\|^2}{\|\hat{T}(p=1)\|^2} \right)^{\frac{1}{2}}, 1 \right] \quad (5)$$

to compare different noisy channels on the same footing. In order to check the entanglement condition (1), we put the correlation tensor of a state (4) in a Schmidt form itself. The general form of the tensor elements is given in Appendix C. Note that the Schmidt form of the state does not imply a diagonal form of the corresponding tensor. Even for a two-qutrit state non-diagonal elements appear. This is not the case for qubits. Because of, the above reason, calculations of  $L_{\max}$  require the diagonalization of the tensor, which is a computationally difficult problem even for small  $d$ .

For white, product, and colored noises we analytically compute the critical parameter  $v_{\text{crit}, ENT}^d$  for the maximally entangled states (diagonal form of the correlation tensor) of a pair of qudits:

$$|\psi_{\max}^d\rangle = \frac{1}{\sqrt{d}} \sum_{i=0}^{d-1} |ii\rangle \quad (6)$$

We present results for arbitrary  $d$  and for  $d \rightarrow \infty$ .

We also analyze all non-maximally entangled pure initial states of qutrits ( $d = 3$ ), parametrized as

$$|\psi^3(\alpha, \beta)\rangle = \cos \alpha |00\rangle + \sin \alpha \sin \beta |11\rangle + \sin \alpha \cos \beta |22\rangle. \quad (7)$$

The study is also done for lower Schmidt rank states, for  $d = 3, 4$ :

$$|\psi_{\text{rank}-k}^d\rangle = \sum_{j=d-k}^{d-1} c_j |jj\rangle, \quad (8)$$

where  $k < d$  and  $\sum_{j=d-k}^{d-1} |c_j|^2 = 1$ .

## 4. Results for various types of noise

### 4.1. White noise

White noise is represented by an admixture of the totally mixed state. A mixture of white noise and two-qudit pure state  $|\psi\rangle$  can be written as

$$\rho_{\text{white}}(v) = v|\psi\rangle\langle\psi| + \frac{1-v}{d^2} \mathbb{1}_d \otimes \mathbb{1}_d. \quad (9)$$

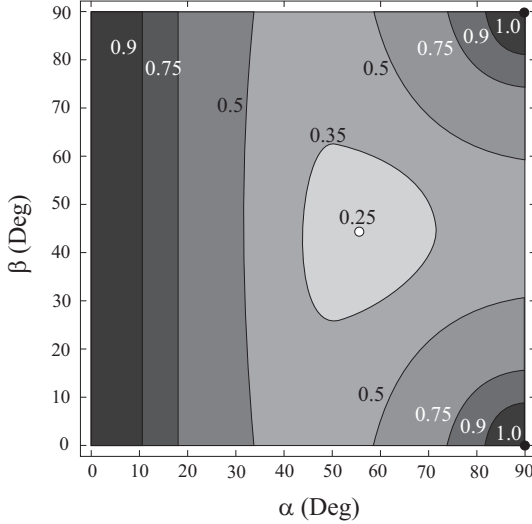


Figure 1: Critical values  $v_{\text{crit, ENT}}^3$  to detect entanglement for two-qutrit non-maximally entangled states (7) and white noise admixture. For  $v > v_{\text{crit, ENT}}^3$ , the state is entangled. The lowest critical value 0.25 is obtained for the maximally entangled state  $|\psi_{\text{max}}^3\rangle$ .

Since white noise has no correlations, the correlation tensor  $\hat{T}(v)$  for the state  $\rho_{\text{white}}(v)$  is given by  $\hat{T}(v) = v\hat{T}$ .

In the case of the maximally entangled state, only diagonal components of the tensor are nonzero and given by  $T_{ii}(v) = \pm v/(d-1)$  for  $i \in \{1, 2, \dots, d^2-1\}$ . Therefore, we have  $L_{\text{max}} = v/(d-1)$  and  $\|\hat{T}(v)\|^2 = v^2(d+1)/(d-1)$ . Using the criterion (1), we can conclude that the state  $\rho_{\text{white}}(v)$  is entangled if  $v > (d+1)^{-1}$ . This recovers the result of Ref. [16]. In the limit of  $d \rightarrow \infty$ , the critical value  $v_{\text{crit, ENT}}^d \rightarrow 0$ .

For two-qutrit non-maximally entangled states (7), we obtain  $L_{\text{max}} = v(8+\sqrt{K})/16$  and  $\|\hat{T}(v)\|^2 = v^2(2-K/64)$ , where  $K = 31 + 12 \cos 2\alpha + 21 \cos 4\alpha + 24 \cos 4\beta \sin^4 \alpha$ . In Fig. 1, we present the critical values  $v_{\text{crit, ENT}}^3$ . As a result, the state (7) is entangled for all  $\alpha$  and  $\beta$  except for  $\alpha = 0$ ,  $\{\alpha = \pi/2, \beta = 0\}$ , and  $\{\alpha = \pi/2, \beta = \pi/2\}$ . The lowest value of  $v_{\text{crit, ENT}}^3 = 0.25$  is obtained by the maximally entangled state  $|\psi_{\text{max}}^3\rangle$ .

We also calculate numerically the critical value  $v_{\text{crit, ENT}}^3$  for lower Schmidt rank states (8);  $|\psi_{\text{rank-2}}^3\rangle = \frac{1}{\sqrt{2}}(|11\rangle + |22\rangle)$ ,  $|\psi_{\text{rank-2}}^4\rangle = \frac{1}{\sqrt{2}}(|22\rangle + |33\rangle)$ , and  $|\psi_{\text{rank-3}}^4\rangle = \frac{1}{\sqrt{3}}(|11\rangle + |22\rangle + |33\rangle)$ . All this is compared with maximally entangled states. The analysis shows that the lower is the Schmidt rank of such states the more fragile is their entanglement. The values are summarized in Table 2 (note that the results  $v_{\text{crit, ENT}}^d$  for white noise are identical to the values  $\xi(p_{\text{crit, ENT}}^d)$  in Eq. (5) for local depolarizing noise which we will show in the next section).

#### 4.2. Local depolarizing noise

A  $d$ -dimensional quantum state exiting a local depolarizing channel is given by

$$\Lambda_r^{\text{depol}}(\rho) = (1-r)\rho + \frac{r}{d}\mathbb{1}. \quad (10)$$

The use of such a formalism gives us a method of estimating how much noise (disturbance) is introduced per qudit. With probability  $1-r$  the initial state  $\rho$  still remain unaltered by the decoherence. To describe the local depolarizing effect on a two-qudit system, one can use the following transformation of the generalized Gell-Mann matrices:

$$\Lambda_r^{\text{depol}}(M_j) = (1-r)M_j, \quad (11)$$

where  $j \in \{1, 2, \dots, d^2-1\}$ , and make the replacement in  $T_{\mu_1\mu_2} = c(d)\text{Tr}[\rho(M_{\mu_1} \otimes M_{\mu_2})]$ .

For the maximally entangled state (6), after such a transformation only diagonal components of the correlation tensor are non-vanishing, and they read

$$T_{ii}(r_1, r_2) = \pm \frac{(1-r_1)(1-r_2)}{(d-1)}, \quad (12)$$

where  $i \in \{1, 2, \dots, d^2-1\}$  and local depolarizing effects on two subsystems are parametrized by  $r_1$  and  $r_2$ . Therefore, we have  $L_{\text{max}} = \frac{(1-r_1)(1-r_2)}{(d-1)}$  and  $\|\hat{T}(r_1, r_2)\|^2 = (1-r_1)^2(1-r_2)^2 \frac{(d+1)}{(d-1)}$ .

Consider the case in which  $r_1 = r_2 = r$  and define  $1-r = p$ . Using the criterion (1), the critical value  $p_{\text{crit, ENT}}^d$  in local depolarized channel is obtained as

$$p_{\text{crit, ENT}}^d = (d+1)^{-\frac{1}{2}}. \quad (13)$$

We see that when  $d \rightarrow \infty$ ,  $p_{\text{crit, ENT}}^d \rightarrow 0$ . Thus with increasing  $d$  the maximal entanglement is more and more resistant with respect to the depolarizing noise.

Our study for arbitrary pure states of two qutrits (7) gives  $L_{\text{max}} = p^2(8+\sqrt{K})/16$  and  $\|\hat{T}(p)\|^2 = p^4(2-K/64)$ . The critical values  $p_{\text{crit, ENT}}^d$  are plotted in Fig. 2. It is entangled for all  $\alpha$  and  $\beta$  except those related to product states:  $\alpha = 0$ ,  $\{\alpha = \frac{\pi}{2}, \beta = 0\}$  and  $\{\alpha = \frac{\pi}{2}, \beta = \frac{\pi}{2}\}$ . The lowest value of  $p_{\text{crit, ENT}}^3 = 0.5$  is obtained by the maximally entangled state. In Table 1, we give numerical results of the critical values  $p_{\text{crit, ENT}}^d$  for lower Schmidt rank states (8). For a specific dimension, entangled states of lower Schmidt rank are less resistant to local depolarizing noise than entangled states of higher Schmidt rank.

For local depolarizing channel and maximally entangled states, we obtain  $\|\hat{T}(p_{\text{crit, ENT}}^d)\|^2 = \frac{1}{d^2-1}$  and  $\|\hat{T}(p=1)\|^2 = \frac{d+1}{d-1}$ . This yields  $\xi(p_{\text{crit, ENT}}^d) = \frac{1}{d+1}$ , which is equivalent to  $\xi(p_{\text{crit, ENT}}^d)$  for white noise. In that sense, the local depolarizing noise for the case  $r_1 = r_2 = r$  and white noise show the equivalent decoherence phenomena (noise robustness) to the entanglement.

For  $r_1 \neq r_2$ , if we replace  $1-r_1$  by  $p_1$  and  $1-r_2$  by  $p_2$ , respectively and we define the product of  $p_1$  and  $p_2$  as a critical parameter  $p_{\text{crit, ENT}}^d$  of detecting entanglement, then the entanglement criterion (1) yields

$$p_{\text{crit, ENT}}^d = p_1 p_2 = \frac{1}{d+1}. \quad (14)$$

Hence, satisfying the condition (14), we can obtain a set of feasible solutions for  $r_1$  and  $r_2$  between 0 and  $\frac{d}{d+1}$ .

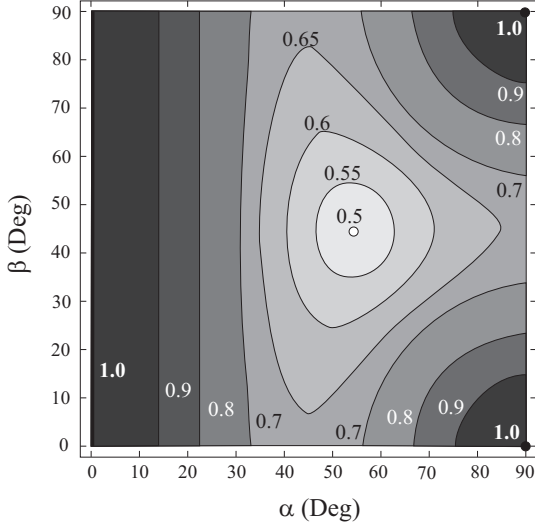


Figure 2: Critical values  $p_{\text{crit},\text{ENT}}^3$  for entanglement detection are shown for two-qutrit non-maximally entangled state under local depolarizing noise. The lowest critical value 0.5 is achieved by the maximally entangled state  $|\psi_{\text{max}}^3\rangle$ .

#### 4.3. Product noise

We consider the following output states:

$$\rho_{\text{prod}}(v) = v|\psi\rangle\langle\psi| + (1-v)\rho_a \otimes \rho_b, \quad (15)$$

where  $\rho_i = \sum_{j=0}^{d-1} |c_j|^2 |j\rangle_i\langle j|$  is the reduced density matrix of the  $i$ th subsystem. The critical values  $v_{\text{crit},\text{ENT}}^3$  are presented in Fig. 3. The lowest critical value  $v_{\text{crit},\text{ENT}}^3 = 0.25$  is also obtained by the maximally entangled state  $|\psi_{\text{max}}^3\rangle$ . This is due to the fact that the product noise is reduced to the white noise. Note that  $v_{\text{crit},\text{ENT}}^3 = 1$  for product states, whereas in the limits  $\alpha \rightarrow 0$ ,  $\{\alpha \rightarrow \pi/2, \beta \rightarrow 0\}$ , or  $\{\alpha \rightarrow \pi/2, \beta \rightarrow \pi/2\}$ , the state (15) is entangled for the critical visibility approaching 0.6039. In other words, our geometrical method is very sensitive in the presence of product noise.

#### 4.4. Colored product noise

In the special case of output states

$$\rho_c(v) = v|\psi_{\text{max}}^d\rangle\langle\psi_{\text{max}}^d| + (1-v)\hat{\pi}_c \otimes \hat{\pi}_c, \quad (16)$$

with  $\hat{\pi}_c = |d-1\rangle\langle d-1|$ , the correlation tensor of the state (16) has the following non-vanishing components:

$$T_{ii}(v) = \begin{cases} \pm \frac{v}{d-1} & \text{for } i \in \{1, \dots, d^2-2\}, \\ 1 - \frac{v(d-2)}{d-1} & \text{for } i = d^2-1. \end{cases} \quad (17)$$

In order to obtain more efficient entanglement condition, we consider a generalized version of the criterion (1) as

$$\max_{\hat{T}_{\text{prod}}} (\hat{T}, \hat{T}_{\text{prod}})_G < \|\hat{T}\|_G^2. \quad (18)$$

Here the scalar product is defined by a positive semidefinite diagonal metric  $G$  [8]:

$$(\hat{X}, \hat{Y})_G = \sum_{i,j=1}^{d^2-1} X_{ij} G_{ij} Y_{ij}. \quad (19)$$

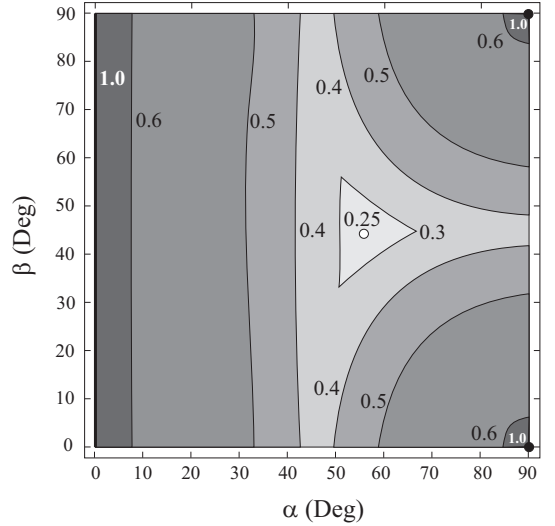


Figure 3: Critical values  $v_{\text{crit},\text{ENT}}^3$  for indicating entanglement with product noise. For  $\alpha \rightarrow 0$ ,  $\{\alpha \rightarrow \pi/2, \beta \rightarrow 0\}$ , and  $\{\alpha \rightarrow \pi/2, \beta \rightarrow \pi/2\}$ , the state (15) is entangled for the critical visibility approaching 0.6039.

We consider a diagonal metric  $G$  with the following nonzero elements:  $G_{ii} = 1$  for  $i \in \{1, 2, \dots, d^2-2\}$  and  $G_{d^2-1, d^2-1} = v$ . With such a metric, the left-hand side of (18) reads  $L_{\text{max}}^G = v[1 - v(d-2)/(d-1)]$  and  $\|\hat{T}(v)\|_G^2 = v[1 + v(-6 + 6d - d^2 + v(d-2)^2)/(d-1)^2]$ . For  $d \geq 2$ ,  $\|\hat{T}(v)\|_G^2$  is always greater than  $L_{\text{max}}^G$ . It implies that the state  $\rho_c(v)$  is always entangled except  $v = 0$ , i.e., even for an infinitesimally small  $v$  the state is entangled.

#### 4.5. Amplitude damping noise

An amplitude damping channel can be described by a process of energy dissipation of a quantum system to environment. The transition of excitation occurs between excited state and the ground state with a finite probability. Here we consider a model that no transition is allowed between excited states. Such an amplitude damping channel can be described by

$$\rho_{\text{AD}}(r) = \sum_{k,m=0}^{d-1} E_k(r) \otimes E_m(r) \rho(E_k(r) \otimes E_m(r))^\dagger, \quad (20)$$

where

$$E_0 = |0\rangle\langle 0| + \sqrt{1-r} \sum_{i=1}^{d-1} |i\rangle\langle i|, \\ E_j = \sqrt{r} |0\rangle\langle j|, \quad j \in \{1, 2, \dots, d-1\}. \quad (21)$$

The transformation of the generalized Gell-Mann matrices is given by

$$M_j(r) = \begin{cases} \sqrt{1-r} M_j & \text{for } M_j \in \{M_{1,k}^{s(\text{or } a)}\} \\ (1-r) M_j & \text{otherwise,} \end{cases} \quad (22)$$

where  $j \in \{1, 2, \dots, d^2-1\}$ ,  $k \in \{2, 3, \dots, d\}$ , the  $M_{1,k}^{s(\text{or } a)}$  is the symmetric (or antisymmetric) Gell-Mann matrices

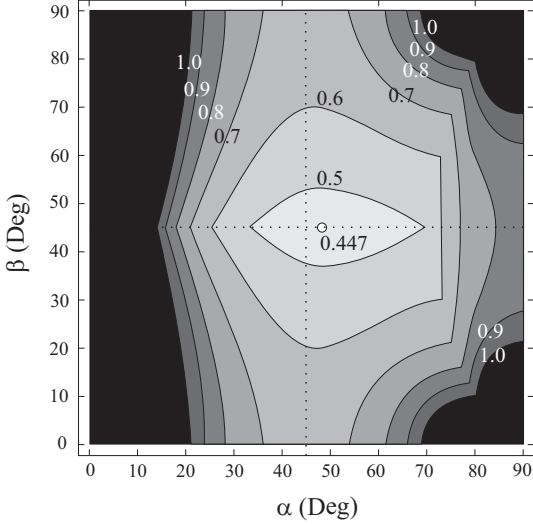


Figure 4: We show the critical value  $p_{\text{crit},\text{ENT}}^3$  of entanglement identification for non-maximally entangled state for amplitude damping noise. The lowest value ( $\approx 0.447$ ) is obtained for the state  $|\psi(\frac{4\pi}{15}, \frac{\pi}{4})\rangle$  of (7).

(see Appendix A for details). Here, we do not consider the transformation rule for the diagonal Gell-Mann matrices as they are redundant in later calculation.

For the maximally entangled states, we have the following nonzero components of the correlation tensor

$$T_{ii}(r) = \begin{cases} \pm \frac{(1-r)}{(d-1)} & \text{for } M_i \in \{M_{1,k}^s \text{ or } a\} \\ \pm \frac{(1-r)^2}{(d-1)} & \text{otherwise,} \end{cases} \quad (23)$$

where  $i \in \{1, 2, \dots, d^2 - d\}$ . Although  $T_{ij}(r)$  are nonzero for  $i, j \in \{d^2 - d, d^2 - d + 1, \dots, d^2 - 1\}$ , still they do not have any impact in our calculation to obtain the *sufficient* condition for entanglement. More precisely, to calculate the critical values with a *specific* combination of components of correlation tensor, we use the generalized criterion (18) involving the diagonal metric;  $G_{ii} = 1$  for  $i \in \{1, 2, \dots, d^2 - d\}$  and other components are zero. As a result, we have  $L_{\max} = (1-r)/(d-1)$  and  $\|\hat{T}(r)\|^2 = (1-r)^2 [2 + (d-2)(1-r)^2]/(d-1)$ . Thus, the entanglement criterion (18) reduces to  $(d-2)p^3 + 2p > 1$ , where  $p = 1-r$ . We find that for  $d > 2$  the state is entangled if the value  $p$  exceeds the critical value

$$p_{\text{crit},\text{ENT}}^d = \left( \frac{1}{2(d-2)} \right)^{1/3} \left( 1 - \frac{A^{1/3}}{B^2} \right) B, \quad (24)$$

where  $A = 2^5/[3^3(d-2)]$  and  $B = [1 + (1+A)^{1/2}]^{1/3}$ . The critical value  $p_{\text{crit},\text{ENT}}^d$  goes to zero when  $d \rightarrow \infty$ .

It is worth noting that non-maximally entangled states for  $d = 3, 4$  in Eq. (7) are more robust than the maximally entangled state (6) against this type of noise. The corresponding non-maximally entangled states are  $|\psi(\frac{4\pi}{15}, \frac{\pi}{4})\rangle$  for  $d = 3$  and  $|\psi_{\text{nmax}}^4\rangle = \cos(0.853)|00\rangle + \sin(0.853)(|11\rangle + |22\rangle + |33\rangle)/\sqrt{3}$ . The critical values  $p_{\text{crit},\text{ENT}}^3$  are plotted in Fig. 4. In Table 1, we show numerical results of the critical values  $p_{\text{crit},\text{ENT}}^d$  for lower Schmidt rank states (8) for

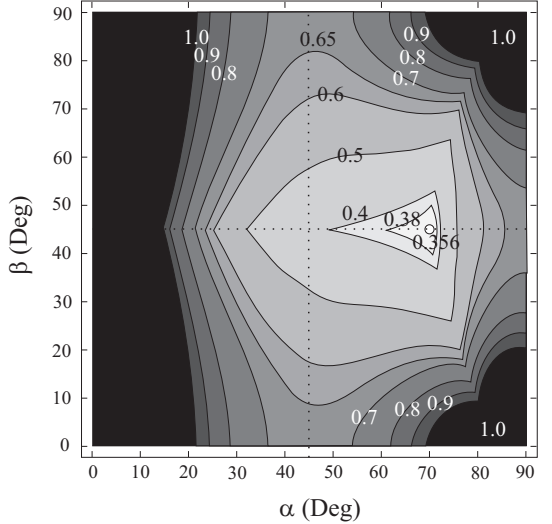


Figure 5: We show the critical value  $\xi(p_{\text{crit},\text{ENT}}^3)$  of entanglement identification for non-maximally entangled state for amplitude damping noise. The lowest value (0.3560) for  $p_{\text{crit},\text{ENT}}^3$  is obtained for the non-maximally entangled state  $|\psi(\frac{7\pi}{18}, \frac{\pi}{4})\rangle$  of (7).

$d = 3, 4$ . It is found that the maximally entangled states of lower Schmidt rank are less robust than the maximally entangled states of higher Schmidt rank. As a matter of fact the positive semidefinite diagonal metric  $G$  is not unique, one might be able to obtain lower values for  $p_{\text{crit},\text{ENT}}^d$  than our results.

We check critical parameter  $\xi(p_{\text{crit},\text{ENT}}^d)$  for the maximally entangled state. Here  $\|\hat{T}(p_{\text{crit},\text{ENT}}^d)\|^2 = \frac{(p_{\text{crit},\text{ENT}}^d)^2}{d-1} [2 + (d-2)(p_{\text{crit},\text{ENT}}^d)^2]$  and  $\|\hat{T}(p=1)\|^2 = \frac{d}{d-1}$  which yields  $\xi(p_{\text{crit},\text{ENT}}^d) = p_{\text{crit},\text{ENT}}^d (2 + (d-2)(p_{\text{crit},\text{ENT}}^d)^2)^{\frac{1}{2}} d^{-\frac{1}{2}}$ . Hence,  $\xi(p_{\text{crit},\text{ENT}}^d) \rightarrow 0$ , when  $d \rightarrow \infty$ . Due to our entanglement criterion we obtain lower value for  $\xi(p_{\text{crit},\text{ENT}}^3)$  for a specific non-maximally entangled state than the maximally entangled state while analyzing for amplitude damping noise. The corresponding non-maximally entangled state is  $|\psi(\frac{7\pi}{18}, \frac{\pi}{4})\rangle$  for  $d = 3$ , and we obtain  $p_{\text{crit},\text{ENT}}^3 = 0.4990$ . The critical values  $\xi(p_{\text{crit},\text{ENT}}^3)$  are plotted in Fig. 5. Comparisons between  $v_{\text{crit},\text{ENT}}^d$  and  $\xi(p_{\text{crit},\text{ENT}}^d)$ , calculated for white or local depolarizing noise and amplitude damping noise, respectively are shown in Table 2.

## 5. Testing Entanglement with Bell inequalities

In this section, we analyze noise resistance of violation of Bell-type inequalities for the bipartite quantum states. To this end, we employ the CGLMP inequality introduced in Ref. [15], which can be written as

$$I_d = \sum_{k=0}^{\lfloor \frac{d}{2} \rfloor - 1} \left( 1 - \frac{2k}{d-1} \right) (\mathcal{B}_k - \mathcal{B}_{-(k+1)}) \leq 2, \quad (25)$$

where  $\mathcal{B}_k = P(A_1 = B_1 + k) + P(B_1 = A_2 + k + 1) + P(A_2 = B_2 + k) + P(B_2 = A_1 + k)$ .

Table 1: Summary of the critical values  $p_{\text{crit}, ENT}^d$  to detect entanglement for the various bipartite states under depolarizing and amplitude damping noises: the maximally entangled state  $|\psi_{\text{max}}^d\rangle$ , the non-maximally entangled state  $|\psi_{\text{nmax}}^d\rangle$ , and the lower Schmidt rank states  $|\psi_{\text{rank-}k}^d\rangle$ . For amplitude damping noise, the specific non-maximally entangled states present lower critical value  $p_{\text{crit}, ENT}^d$  than the maximally entangled ones. The specific states are presented below Eq. (24).

| noise              | $d$ | $ \psi_{\text{max}}^d\rangle$ | $ \psi_{\text{rank-}2}^d\rangle$ | $ \psi_{\text{rank-}3}^d\rangle$ | $ \psi_{\text{nmax}}^d\rangle$ |
|--------------------|-----|-------------------------------|----------------------------------|----------------------------------|--------------------------------|
| local depolarizing | 2   | 0.5773                        | -                                | -                                | -                              |
|                    | 3   | 0.5                           | 0.6546                           | -                                | -                              |
|                    | 4   | 0.4472                        | 0.6794                           | 0.5283                           | -                              |
| amplitude damping  | 2   | 0.5                           | -                                | -                                | -                              |
|                    | 3   | 0.4534                        | 0.8165                           | -                                | 0.4465                         |
|                    | 4   | 0.4239                        | 0.8660                           | 0.6124                           | 0.4074                         |

Table 2: A summary of the critical values  $\xi(p_{\text{crit}, ENT}^d)$  for local depolarizing noises and amplitude damping noise in detection of entanglement for  $|\psi_{\text{max}}^d\rangle$  and the lower Schmidt rank states  $|\psi_{\text{rank-}k}^d\rangle$ . Note that the values  $\xi(p_{\text{crit}, ENT}^d)$  for local depolarizing noise are identical to  $v_{\text{crit}, ENT}^d$  for white noise. For amplitude damping noise, the specific non-maximally entangled state  $|\psi(\frac{7\pi}{18}, \frac{\pi}{4})\rangle$  for  $d = 3$  presents lower critical values  $\xi(p_{\text{crit}, ENT}^3)$  than the maximally entangled one.

| noise              | $d$ | $ \psi_{\text{max}}^d\rangle$ | $ \psi_{\text{rank-}2}^d\rangle$ | $ \psi_{\text{rank-}3}^d\rangle$ | $ \psi_{\text{nmax}}^d\rangle$ |
|--------------------|-----|-------------------------------|----------------------------------|----------------------------------|--------------------------------|
| local depolarizing | 2   | 0.3333                        | -                                | -                                | -                              |
|                    | 3   | 0.25                          | 0.4285                           | -                                | -                              |
|                    | 4   | 0.2                           | 0.4615                           | 0.2790                           | -                              |
| amplitude damping  | 2   | 0.5                           | -                                | -                                | -                              |
|                    | 3   | 0.3888                        | 0.6667                           | -                                | 0.3560                         |
|                    | 4   | 0.3256                        | 0.750                            | 0.3750                           | -                              |

We compare robustness of violation of the CGLMP inequality with respect to different noisy channels for the maximally entangled state  $|\psi_{\text{max}}^d\rangle$ . In [15], the robustness to white noise by the same state are considered.

### 5.1. White noise

We give an analytical solution for the critical visibility to violate the inequality (25) with the maximally entangled states and then consider the case for  $d \rightarrow \infty$ .

Since the white noise does not contribute to the violation of the CGLMP inequality, the quantum value for the state  $\rho_{\text{white}}(v)$  in Eq. (9) is given by

$$I_{QM}^d[\rho_{\text{white}}(v)] = v I_{QM}^d[|\psi\rangle]. \quad (26)$$

Therefore the critical parameters are given by

$$v_{\text{crit}, LR}^d = 2/I_{QM}^d[|\psi\rangle], \quad (27)$$

and equal:  $v_{\text{crit}, LR}^2 \approx 0.7073$ ,  $v_{\text{crit}, LR}^3 \approx 0.6962$ ,  $v_{\text{crit}, LR}^4 \approx 0.6906$  and  $v_{\text{crit}, LR}^\infty \approx 0.6734$  [15]. Note that the lowest critical visibility is achieved by non-maximally entangled states [18] and studied in details (for  $d = 3$ ) in Ref. [19]: the value is  $v_{\text{crit}, LR}^3 = 0.6861$  (refer to Ref. [19]) and the state is  $|\psi^3(1.0601, 0.7854)\rangle$  [see (7)]. Note that such specific non-maximally entangled state shows the critical value for entanglement as  $v_{\text{crit}, ENT}^3 = 0.2883$ .

Table 3: The critical parameters to indicate violation of CGLMP inequality  $p_{\text{crit}, LR}^d$  are calculated for local depolarizing and amplitude damping noises for the bipartite maximally entangled state in higher dimensional systems.

| $d$      | depolarizing | amplitude damping |
|----------|--------------|-------------------|
| 2        | 0.8410       | 0.7071            |
| 3        | 0.8344       | 0.7468            |
| 4        | 0.8310       | 0.7647            |
| 5        | 0.8290       | 0.7750            |
| 10       | 0.8248       | 0.7954            |
| $\infty$ | 0.8206       | 0.8206            |

### 5.2. White noise treated as local depolarizing channel

Following the transformation rules for the Gell-Mann matrices shown in Eq. (11), the maximally entangled state  $|\psi_{\text{max}}^d\rangle$  after local depolarizing channel can be written as

$$\rho_{\text{depol}}(r) = (1-r)^2 |\psi_{\text{max}}^d\rangle\langle\psi_{\text{max}}^d| + \frac{r(2-r)}{d^2} \mathbb{1}_d \otimes \mathbb{1}_d. \quad (28)$$

Similarly to the white noise, no contribution from the noise part to the Bell expression (25), then the critical parameters for the violation read

$$p_{\text{crit}, LR}^d = \sqrt{2/I_{QM}^d[|\psi\rangle]}, \quad (29)$$

where  $p_{\text{crit}, LR}^d = (1 - r_{\text{crit}, LR}^d)$ . The results are given in Table 3. However, in terms of visibility  $v_{\text{crit}, LR}^d$ , the result is identical with (27).

### 5.3. Colored noise

We check the violation of CGLMP inequality by the maximally entangled state mixed with colored noise of (16). Numerically for  $d = 3$  we find that if we choose generalized  $SU(3)$  transformation matrix instead of choosing settings (D.1), then CGLMP inequality (25) is violated whenever  $v > 0$ .

### 5.4. Amplitude damping channel

After amplitude damping channel (20), the maximally entangled state is given by

$$\begin{aligned} \rho_{\text{AD}}(r) = & \frac{1+r^2(d-1)}{d} |00\rangle\langle 00| + \frac{(1-r)^2}{d} \sum_{m,k \neq 0}^{d-1} |mm\rangle\langle kk| \\ & + \frac{(1-r)}{d} \left[ \sum_{m \neq 0}^{d-1} |mm\rangle\langle 00| + \sum_{k \neq 0}^{d-1} |00\rangle\langle kk| \right] \\ & + \frac{r(1-r)}{d} \left[ \sum_{m \neq 0}^{d-1} |m0\rangle\langle m0| + \sum_{k \neq 0}^{d-1} |0k\rangle\langle 0k| \right]. \end{aligned} \quad (30)$$

We numerically check the critical parameters for  $d = 2, 3, 4, 5$ , and 10. The results are given in Table 3.

We see that the critical parameter increases with the dimension. It has a tendency to attain saturation for very

large  $d$ . We give an analytical result for  $d$  tends to  $\infty$  in Appendix D. Note that for  $d = 3$  the lowest critical visibility ( $p_{\text{crit},LR}^3 = 0.7316$ ) to violate the CGLMP inequality is obtained by non-maximally entangled state  $|\psi^3(0.8730, 0.6449)\rangle$  [see (7)]. We check that such entangled state reads the critical value  $p_{\text{crit},ENT}^3 = 0.5$  for entanglement detection, and  $\xi(p_{\text{crit},ENT}^3) = 0.4513$ , which are larger than the lowest values (see Tables 1 and 2). To compare, we also check  $p_{\text{crit},LR}^3$  for the violation of the inequality with a different non-maximally entangled state  $|\psi^3(\frac{4\pi}{15}, \frac{\pi}{4})\rangle$ , which gives the lowest  $p_{\text{crit},ENT}^3$ . It reads  $p_{\text{crit},LR}^3 = 0.7429$ . Furthermore, we extend our calculation by checking  $p_{\text{crit},LR}^3$  for the non-maximally state  $|\psi^3(\frac{7\pi}{18}, \frac{\pi}{4})\rangle$  which shows the lowest  $\xi(p_{\text{crit},ENT}^3)$ . The value reads  $p_{\text{crit},LR}^3 = 0.8640$ .

Although we obtain a different tendency of the critical values  $p_{\text{crit},LR}^d$  between local depolarizing and amplitude damping noises in lower dimensions, for  $d \rightarrow \infty$  they show the same values (see Table 3).

### 5.5. Fidelity of quantum states with critical noise

In this section we give analytic expression of fidelity, i.e., the measure of closeness between two quantum states, e.g., the state after noisy channel with the pure state (here we only consider the maximally entangled state) of the system under investigation.

Usually fidelity  $F$  for two quantum states is defined as  $\sqrt{\langle\phi|\rho|\phi\rangle}$ , where  $\phi$  is a pure state whereas  $\rho$  is a mixed state. We consider the maximally entangled state (6) as  $\phi$ , and  $\rho$  is parametrized by critical parameters  $v_{\text{crit},LR}^d$  for white noise and  $r_{\text{crit},LR}^d$  for local depolarizing and amplitude damping noises. The general form of  $\rho$ 's are given in Eqs. (9), (28), and (30) for white, local depolarizing, and amplitude damping channels, respectively. The critical fidelities ( $F_{\text{crit},LR}^d$ ) for white, local depolarizing, and amplitude damping are  $(v_{\text{crit},LR}^d + \frac{1-v_{\text{crit},LR}^d}{d^2})^{\frac{1}{2}}$ ,  $((1-r_{\text{crit},LR}^d)^2 + \frac{r_{\text{crit},LR}^d(2-r_{\text{crit},LR}^d)}{d^2})^{\frac{1}{2}}$ , and  $\frac{1}{d}(1+(d-1)((1-r_{\text{crit},LR}^d)^2 + 1) + (d-1)^2(1-r_{\text{crit},LR}^d)^2)^{\frac{1}{2}}$ , respectively.

To show comparison between critical values of fidelity for different noises we present our results for specific dimensions in Table 4. We obtain identical values for  $F_{\text{crit},LR}^d$  for white and local depolarizing channel but it differs with critical fidelity parameter for amplitude damping noise in lower dimension.

### 5.6. Werner gap

A “Werner gap” explains the differences of parameters characterizing entanglement and violation of Bell inequalities for mixed entangled states [16, 17]. Here, such gap reads  $W = p_{\text{crit},LR}^d - p_{\text{crit},ENT}^d$ . In Table 5, we compare the values for the mixtures of local depolarizing and amplitude damping channels with maximally entangled states for  $d = 2, 3, 4$ , and  $\infty$ . In the previous Sections 4.2 and 4.5, we find that, when  $d \rightarrow \infty$ ,  $p_{\text{crit},ENT}^d \rightarrow 0$  for both noisy

Table 4: Critical fidelity  $F_{\text{crit},LR}^d$  is calculated for white, local depolarizing and amplitude damping noises for the maximally entangled state. White and local depolarizing noises show the same values of  $F_{\text{crit},LR}^d$ .

| $d$      | local depolarizing | amplitude damping |
|----------|--------------------|-------------------|
| 2        | 0.8834             | 0.8660            |
| 3        | 0.8544             | 0.8397            |
| 4        | 0.8426             | 0.8298            |
| $\infty$ | 0.8206             | 0.8206            |

Table 5: Werner gap  $W = (p_{\text{crit},LR}^d - p_{\text{crit},ENT}^d)$  is calculated for local depolarizing and amplitude damping noises for the maximally entangled state.

| $d$      | local depolarizing | amplitude damping |
|----------|--------------------|-------------------|
| 2        | 0.2637             | 0.2071            |
| 3        | 0.3344             | 0.2934            |
| 4        | 0.3838             | 0.3408            |
| $\infty$ | 0.8206             | 0.8206            |

channels. However,  $p_{\text{crit},LR}^d$  increases with the increase of the dimension of the system for amplitude damping noise and decreases with the increase of the dimension for depolarizing noise (see the Table 3). As a result, the overall effect reads that the discrepancy between  $p_{\text{crit},LR}^d$  and  $p_{\text{crit},ENT}^d$  increases with the dimension. Therefore, the result justifies the known fact that not all states, which are entangled, violate specific Bell inequalities (in this case CGLMP inequality).

## 6. Conclusions

We analyze a noise resistance for entanglement of bipartite qudit systems. We construct entanglement indicators by means of a difference of geometrical property of correlation tensors of separable and entangled states. It is worth mentioning that to test whether the state is entangled, it is sufficient to break the threshold, i.e., it is not required to measure all correlations. To this end, we introduce different forms of positive semidefinite diagonal metric  $G$  to accumulate optimal components of correlation tensors. The correlation tensors are parametrized by a set of parameters;  $v_{\text{crit},ENT}^d$ ,  $p_{\text{crit},ENT}^d$ , and  $\xi(p_{\text{crit},ENT}^d)$ . We provide analytical as well as numerical calculations of critical values of noise parameters for various bipartite states.

We also investigate a violation of CGLMP inequality and its critical values, and compare them with the results for entanglement. It is interesting to note that there exists a finite difference (Werner gap) even for the case, where  $d \rightarrow \infty$ . Hence, one can construct local hidden variable models for the two-qudit mixed entangled states in the range of the gap.

In addition, we compute critical fidelity  $F_{\text{crit},LR}^d$  to quantify violation of local realism. For local depolarizing and amplitude damping channels, the critical fidelity

to violate CGLMP inequality decreases as the dimensions of the systems are increased. Thus, as we increase the dimensions of the systems, the tolerance of noise admixture for the optimal maximally entangled states increases. However, for  $d \rightarrow \infty$  the critical fidelity reaches 0.8206 for both channels.

At the end, it is worth to make few comments on the entanglement criterion with amplitude damping noise. Because of the specific type of entanglement indicator, we may obtain a set of values  $p_{\text{crit},\text{ENT}}^d$ , and  $\xi(p_{\text{crit},\text{ENT}}^d)$ , which are lower for different non-maximally entangled states than the maximally entangled ones of arbitrary dimensions. We explicitly check the case for  $d = 3$ .

It will also be interesting to investigate if it can be possible to detect entanglement for lower values of  $p_{\text{crit},\text{ENT}}^d$ , and  $\xi(p_{\text{crit},\text{ENT}}^d)$ , using either the condition (1) or (18) for different types of amplitude damping channels with different types of Kraus operator representations than the certain type used in this work. The study may lead to better entanglement conditions than the one presented here.

## Acknowledgments

AD was initially supported within the International PhD Project “Physics of future quantum-based information technologies”: grant MPD/2009-3/4 of Foundation for Polish Science. WL is supported by NCN Grant No. 2012/05/E/ST2/02352. MZ and JR are supported by TEAM project of FNP. AD and JR acknowledge support of BRISQ2 VII FP EU project. JR also acknowledges the National Research Foundation and Ministry of Education in Singapore.

## Appendix A. Generalized Gell-Mann matrices

The generalized Gell-Mann matrices in an arbitrary dimension  $d$  are the generators of the Lie algebra associated to the special unitary group  $\text{SU}(d)$ . Let  $\lambda_{j,k}$  denote a matrix with a 1 in the  $(j,k)$ -th entry and 0 elsewhere. This leads one to define three groups of matrices: (a) symmetric group;  $M_{j,k}^s = \lambda_{j,k} + \lambda_{k,j}$  for  $1 \leq j < k \leq d$ . (b) antisymmetric group;  $M_{j,k}^a = -i(\lambda_{j,k} - \lambda_{k,j})$  for  $1 \leq j < k \leq d$ . (c) diagonal group;  $M_l^d = \sqrt{\frac{2}{l(l+1)}}(\sum_{j=1}^l \lambda_{j,j} - l\lambda_{l+1,l+1})$  for  $1 \leq l \leq d-1$ . The elements of three groups compose the generators of  $\text{SU}(d)$  group as  $\mathcal{M} = \{M_{1,2}^s, M_{1,3}^s, \dots, M_{1,2}^a, M_{1,3}^a, \dots, M_1^d, \dots, M_{d-1}^d\}$ . For an arbitrary dimension  $d$ , the total number of Gell-Mann matrices is  $d^2 - 1$ . For simplicity, we re-index the elements of the above set as  $\mathcal{M} = \{M_1, M_2, \dots, M_{d^2-1}\}$ . The components satisfy the relations of tracelessness as  $\text{Tr}(M_j) = 0$  and orthogonality as  $\text{Tr}(M_i M_j) = 2\delta_{ij}$ . For example, for

$d = 3$  the set  $\mathcal{M}$  is given by

$$\begin{aligned} M_1 &= \begin{pmatrix} 0 & 1 & 0 \\ 1 & 0 & 0 \\ 0 & 0 & 0 \end{pmatrix}, \quad M_2 = \begin{pmatrix} 0 & 0 & 1 \\ 0 & 0 & 0 \\ 1 & 0 & 0 \end{pmatrix}, \\ M_3 &= \begin{pmatrix} 0 & 0 & 0 \\ 0 & 0 & 1 \\ 0 & 1 & 0 \end{pmatrix}, \quad M_4 = \begin{pmatrix} 0 & -i & 0 \\ i & 0 & 0 \\ 0 & 0 & 0 \end{pmatrix}, \\ M_5 &= \begin{pmatrix} 0 & 0 & -i \\ 0 & 0 & 0 \\ i & 0 & 0 \end{pmatrix}, \quad M_6 = \begin{pmatrix} 0 & 0 & 0 \\ 0 & 0 & -i \\ 0 & i & 0 \end{pmatrix}, \\ M_7 &= \begin{pmatrix} 1 & 0 & 0 \\ 0 & -1 & 0 \\ 0 & 0 & 0 \end{pmatrix}, \quad M_8 = \begin{pmatrix} \frac{1}{\sqrt{3}} & 0 & 0 \\ 0 & \frac{1}{\sqrt{3}} & 0 \\ 0 & 0 & -\frac{2}{\sqrt{3}} \end{pmatrix}, \end{aligned} \quad (\text{A.1})$$

where the first three matrices,  $M_1, M_2$  and  $M_3$ , are symmetric matrices,  $M_4, M_5$  and  $M_6$  are antisymmetric matrices, and  $M_7$  and  $M_8$  are diagonal matrices.

## Appendix B. Calculation of coefficient $c(d)$

A single qudit density matrix is characterized by  $(d^2 - 1)$  dimensional real vector as

$$\rho = \frac{1}{d} \left( \mathbb{1}_d + k \sum_{i=1}^{d^2-1} \rho_i M_i \right), \quad (\text{B.1})$$

where  $\rho_i = \text{Tr}(\rho M_i)$  and we call  $\vec{\rho} = (\rho_1, \dots, \rho_{d^2-1})$  a Generalized Bloch vector, and  $k$  is a normalization coefficient that results in  $|\vec{\rho}| = 1$  for pure state. One can obtain the coefficient  $k = \sqrt{d(d-1)/2}$  as follows: for pure state,  $\text{Tr}(\rho^2) = 1/d + 2k^2|\vec{\rho}|^2/d^2 = 1$ . Therefore, the coefficient is given by  $k = \sqrt{d(d-1)/2}$ . Then, the element of correlation tensor for single qudit can be written as  $T_j = \frac{d}{2} \sqrt{\frac{2}{d(d-1)}} \text{Tr}[\rho M_j] = \sqrt{\frac{d}{2(d-1)}} \text{Tr}[\rho M_j]$ . Therefore the coefficient  $c(d)$  for bipartite state is given by  $c(d) = \frac{d}{2(d-1)}$ .

## Appendix C. Correlation tensor for arbitrary bipartite state

Here, we present a detailed form of elements of the correlation tensor for two-qudit states:  $|\psi\rangle = \sum_{n=0}^{d-1} \alpha_n |nn\rangle$ . As previously mentioned in Sec. 2, the element of correlation tensor is given by  $T_{ij} = c(d) \text{Tr}[\rho(M_i \otimes M_j)]$ , where  $M_i$  is the generalized Gell-Mann matrix presented in Appendix A. Here we do not consider the case where the elements of correlation tensor denote single particle correlation. We can divide the correlation tensor into two parts as follows;

$$\hat{T} = c(d) \begin{pmatrix} \hat{T}^A & 0 \\ 0 & \hat{T}^B \end{pmatrix},$$

where the  $\hat{T}^A$  is  $d(d-1) \times d(d-1)$  matrix and its component is obtained by the Gell-Mann matrices in the symmetric and antisymmetric groups in Appendix A. It has only diagonal elements as

$$T_{ii}^A = \pm 2\alpha_j \alpha_k \quad \text{for } i \in \{1, \dots, d(d-1)\},$$

where  $j, k \in \{0, 1, \dots, d-1\}$  and  $j < k$ .

On one hand, the  $(d-1) \times (d-1)$  matrix  $\hat{T}^B$  has not only off-diagonal components but also diagonal ones. They are obtained by the Gell-Mann matrices from the diagonal group. For the sake of simplicity, here, we re-index the elements of the  $\hat{T}^B$  matrix:

$$\begin{aligned} \hat{T}^B &= \begin{pmatrix} T_{d^2-(d-1), d^2-(d-1)}^B & T_{d^2-(d-1), d^2-(d-2)}^B & \dots \\ T_{d^2-(d-2), d^2-(d-1)}^B & \ddots & \\ \vdots & & \\ T_{d^2-1, d^2-(d-1)}^B & \dots & \dots \end{pmatrix} \\ &\rightarrow \begin{pmatrix} T_{1,1}^B & T_{1,2}^B & \dots & T_{1,d-1}^B \\ T_{2,1}^B & \ddots & & \\ \vdots & & & \\ T_{d-1,1}^B & \dots & & T_{d-1,d-1}^B \end{pmatrix}. \end{aligned}$$

Then, each element is given by

$$\begin{aligned} T_{ii}^B &= \frac{2}{i(i+1)} \left( \sum_{n=0}^{i-1} \alpha_n^2 + i^2 \alpha_i^2 \right), \\ T_{ij}^B &= \frac{2}{\sqrt{ij(i+1)(j+1)}} \left( \sum_{n=0}^{i-1} \alpha_n^2 - i \alpha_i^2 \right), \\ T_{ji}^B &= T_{ij}^B, \end{aligned} \quad (\text{C.1})$$

where  $i, j \in \{1, \dots, d-1\}$  and  $i < j$ .

## Appendix D. $I_{QM}^{AD}(d)$ for amplitude damping noise

We choose the identical two measurement settings per party used to show violation of CGLMP inequality [15, 20]. The measurement operators  $A_s$  for Alice and  $B_t$  for Bob have  $d$  possible outcomes with the following eigenvectors:

$$\begin{aligned} |a\rangle_{A,s} &= \frac{1}{\sqrt{d}} \sum_{j=0}^{d-1} \omega^{j(a+\alpha_s)} |j\rangle_A, \\ |b\rangle_{B,t} &= \frac{1}{\sqrt{d}} \sum_{j=0}^{d-1} \omega^{j(-b+\beta_t)} |j\rangle_B, \end{aligned} \quad (\text{D.1})$$

where  $\omega = \exp(2\pi i/d)$ ,  $a, b \in \{0, 1, \dots, d-1\}$  and  $\alpha_1 = 0, \alpha_2 = 1/2, \beta_1 = 1/4$ , and  $\beta_2 = -1/4$ . This can be realized as follows: each one of the two parties first performs unitary operation on their subsystems with only diagonal entries  $\{0, e^{i\frac{2m\pi}{d}}, \dots, e^{i\frac{2m(d-1)\pi}{d}}\}$ , where  $m \in \{\alpha_s, \beta_t\}$ . Then one of them performs a discrete Fourier transform  $U_{FT}$  (the matrix element is written as  $(U_{FT})_{pq} = \frac{1}{\sqrt{d}} e^{\frac{2i\pi pq}{d}}$ )

and other one applies conjugate  $U_{FT}^*$  and at last they measure in their original bases. Experimentally it can be realized by using phase shifter and multi-port beam splitter on each side. Here, we denote  $P_{QM}^{AD}(A_s = a, B_t = b)$  as the joint probability that Alice obtain the outcome  $a$  from the measurement  $A_s$  and Bob obtain the outcome  $b$  by measuring  $B_t$  for a given state  $\rho_{AD}(r)$  in Eq. (30). Then, the joint probability reads

$$\begin{aligned} P_{QM}^{AD}(A_s = a, B_t = b) &= \frac{1 - (d-1)(r-2)r}{d^3} + \frac{(1-r)}{d^3} \\ &\times \left[ (1-r) \sum_{x,y \neq 0}^{d-1} \omega^{(x-y)\gamma} + \frac{2}{d^3} \sum_{p \neq 0}^{d-1} \cos \left( \frac{2\pi p\gamma}{d} \right) \right], \end{aligned} \quad (\text{D.2})$$

where  $\gamma = a - b + \alpha_s + \beta_t$ . After summation, Eq. (D.2) is given by

$$\begin{aligned} P_{QM}^{AD}(A_s = a, B_t = b) &= \frac{1 - (d-1)(r-2)r}{d^3} + \frac{(1-r)}{d^3} \\ &\times \left[ (1-r) \frac{\sin^2 \left( \frac{\pi(d-1)\gamma}{d} \right)}{\sin^2 \left( \frac{\pi\gamma}{d} \right)} + \frac{\sin \left( \frac{\pi(2d-1)\gamma}{d} \right)}{\sin \left( \frac{\pi\gamma}{d} \right)} - 1 \right] \end{aligned} \quad (\text{D.3})$$

To apply this joint probability into the CGLMP inequality in Eq. (25), we follow the definition introduced in Ref. [15]:

$$P(A_s = B_t + k) = \sum_{n=0}^{d-1} P(A_s = n, B_t = n + k \bmod d).$$

Also due to the symmetrical structure, the probability can be computed using simplified definition:

$$\begin{aligned} P_{QM}^{AD}(A_s = B_t + k) &= \sum_{n=0}^{d-1} P_{QM}^{AD}(A_s = n, B_t = n + k) \\ &= dP_{QM}^{AD}(A_s = k, B_t = 0). \end{aligned}$$

This leads to the following relation:

$$\begin{aligned} P_{QM}^{AD}(A_1 = B_1 + k) &= P_{QM}^{AD}(B_1 = A_2 + k + 1) \\ &= P_{QM}^{AD}(A_2 = B_2 + k) \\ &= P_{QM}^{AD}(B_2 = A_1 + k). \end{aligned}$$

Finally, for amplitude damping noise the quantum value of CGLMP inequality in Eq. (25) reads

$$I_{QM}^{AD}(d, r) = 4 \sum_{k=0}^{\lfloor d/2 \rfloor - 1} \left( 1 - \frac{2k}{d-1} \right) [q_k(r) - q_{-(k+1)}(r)] \quad (\text{D.4})$$

where  $q_k(r) = P_{QM}^{AD}(A_1 = B_1 + k)$  and  $\lfloor p \rfloor$  implies the integer part of  $p$ .

Now, we analyze the value of Eq. (D.4) for  $d \rightarrow \infty$ . The probability  $q_k(r)$  reads

$$\begin{aligned} q_k(r) &= \frac{1 - (d-1)(r-2)r}{d^2} + \frac{(1-r)}{d^2} \times \\ &\left[ (1-r) \frac{\sin^2 \left( \frac{\pi(d-1)(k+1/4)}{d} \right)}{\sin^2 \left( \frac{\pi(k+1/4)}{d} \right)} + \frac{\sin \left( \frac{\pi(2d-1)(k+1/4)}{d} \right)}{\sin \left( \frac{\pi(k+1/4)}{d} \right)} - 1 \right]. \end{aligned}$$

In the limit of  $d \rightarrow \infty$ , the only first sine function of  $q_k(r)$  survives and other terms reduce to zero. Finally, we have

$$\begin{aligned} I_{QM}^{AD}(\infty, r) &= \frac{2(1-r)^2}{\pi^2} \sum_{k=0}^{\infty} \left[ \frac{1}{(k+\frac{1}{4})^2} - \frac{1}{(k+\frac{3}{4})^2} \right] \\ &= (1-r)^2 \frac{32 \times \text{Catalan}}{\pi^2} \\ &\simeq 2.9698(1-r)^2, \end{aligned} \quad (\text{D.5})$$

where Catalan's constant is Catalan  $\simeq 0.9159$ .

## References

### References

- [1] R. Horodecki, P. Horodecki, M. Horodecki, and K. Horodecki, Rev. Mod. Phys. 81 (2009) 865.
- [2] O. Gühne, G. Toth, Physics Reports 474 (2009) 1.
- [3] J. I. de Vicente and M. Huber, Phys. Rev. A 84 (2011) 062306.
- [4] W. Laskowski, M. Markiewicz, T. Paterek and M. Żukowski, Phys. Rev. A 84 (2011) 062305.
- [5] W. Laskowski, M. Markiewicz, D. Rousseau, T. Byrnes, K. Kostrzewska, A. Kolodziejek, Phys. Rev. A 92 (2015) 022339.
- [6] M. Huber, F. Mintert, A. Gabriel, and B. C. Hiesmayr, Phys. Rev. Lett. 104 (2010) 210501.
- [7] C. Spengler, M. Huber, S. Brierley, T. Adaktylos, and B. C. Hiesmayr, Phys. Rev. A 86 (2012) 022311.
- [8] P. Badziąg, Ć. Brukner, W. Laskowski, T. Paterek, and M. Żukowski, Phys. Rev. Lett. 100 (2008) 022339.
- [9] A. Sen(De), U. Sen, and M. Żukowski, Phys. Rev. A 68 (2003) 062301.
- [10] A. Cabello, Á. Feito, and A. Lamas-Linares, Phys. Rev. A 72 (2005) 052112.
- [11] M. A. Nielsen and I. L. Chuang, Quantum Computation and Quantum Information (Cambridge University Press, Cambridge, England, 2000).
- [12] W. Laskowski, T. Paterek, Ć. Brukner and M. Żukowski, Phys. Rev. A 81 (2010) 042101.
- [13] A. Chęcińska and K. Wódkiewicz, Phys. Rev. A 76 (2007) 052306.
- [14] J. S. Bell, Physics 1 (1964) 195.
- [15] D. Collins, N. Gisin, N. Linden, S. Massar and S. Popescu, Phys. Rev. Lett. 88 (2002) 040404.
- [16] R. F. Werner, Phys. Rev. A 40 (1989) 4277.
- [17] M. C. Tran, W. Laskowski and T. Paterek, J. Phys. A 47 (2014) 424025.
- [18] A. Acin, T. Durt, N. Gisin, and J. I. Latorre, Phys. Rev. A 65 (2002) 052325.
- [19] J. Gruca, W. Laskowski, M. Żukowski, Phys. Rev. A 85 (2012) 022118.
- [20] T. Durt, D. Kaszlikowski, and M. Żukowski, Phys. Rev. A 64 (2001) 024101.